THE JOURNAL OF BIOLOGICAL CHEMISTRY VOL. 287, NO. 10, pp. 7535–7542, March 2, 2012

Incompatibility between a Pair of Residues from the Pre-M1 Linker and Cys-loop Blocks Surface Expression of the Glycine Receptor*[S]

Received for publication, November 17, 2011, and in revised form, December 31, 2011 Published, JBC Papers in Press, January 20, 2012, DOI 10.1074/jbc.M111.325126

Qiang Shan[‡§1] **and Joseph W. Lynch**[§¶]

From the [‡]*Brain and Mind Research Institute, University of Sydney, Sydney, New South Wales, 2050 Australia and the* [§]*Queensland Brain Institute and* [¶]*School of Biomedical Sciences, University of Queensland, Brisbane, Queensland, 4072 Australia*

Background: Structural basis determining glycine receptor surface expression is barely known.
Results: A pair of positively charged residues from the pre-M1 linker and Cys-loop blocks glycine receptor surface expression.
Conclusion: Compatibility of residues, in close proximity to each other, is essential for glycine receptor surface expression.
Significance: We provide a novel mechanism, *i.e.* residue incompatibility, for explaining mutation-induced reduction in channel surface expression.

Regulation of cell membrane excitability can be achieved either by modulating the functional properties of cell membrane-expressed single channels or by varying the number of expressed channels. Whereas the structural basis underlying single channel properties has been intensively studied, the structural basis contributing to surface expression is less well characterized. Here we demonstrate that homologous substitution of the pre-M1 linker from the β subunit prevents surface expression of the α1 glycine receptor chloride channel. By investigating a series of chimeras comprising α1 and β subunits, we hypothesized that this effect was due to incompatibility between a pair of positively charged residues, which lie in close proximity to each other in the tertiary structure, from the pre-M1 linker and Cys-loop. Abolishing either positive charge restored surface expression. We propose that incompatibility (electrostatic repulsion) between this pair of residues misfolds the glycine receptor, and in consequence, the protein is retained in the cytoplasm and prevented from surface expression by the quality control machinery. This hypothesis suggests a novel mechanism, *i.e.* residue incompatibility, for explaining the mutation-induced reduction in channel surface expression, often present in the cases of hereditary hyperekplexia.

Cell membrane excitability is regulated mainly by ion channels. Ion channels mediate changes in cell membrane excitability by altering either the ability of channels to flux ions or the number of channels functionally expressed in the membrane (*i.e.* the surface expression).

The glycine receptor (GlyR)[2] is a chloride-permeable ion channel, which, upon activation, inhibits cell membrane excitability. Mutations in the human GlyR cause hereditary hyperekplexia (or startle disease), which is characterized by exaggerated startle reflexes and hypertonia in response to sudden, unexpected auditory or tactile stimuli (1). Hereditary hyperekplexia-causing mutations impair either the function of the expressed single channels or their surface expression, or both. Whereas the structural basis underlying GlyR single channel properties has been intensively studied, the structural basis underlying alterations in its surface expression has been barely investigated (2).

The GlyR, together with several other postsynaptic neurotransmitter receptors including the nicotinic acetylcholine receptor (nAChR), the 5-hydroxytryptamine type-3 receptor ($5HT_3R$), and the type-A γ-aminobutyric acid receptor ($GABA_AR$), belong to the Cys-loop receptor ligand-gated ion channel superfamily, because they share common structural and functional characteristics (2–4). Functional members of this superfamily exist as pentamers. Each subunit is composed of an N-terminal extracellular domain (ECD), a four α-helical transmembrane domain (TMD) bundle and a large intracellular domain. The ECDs incorporate agonist binding sites at subunit interfaces, which are formed by loops A, B, and C from the (+) subunit interface and loops D, E, and F from the (−) subunit interface. The four α-helices (M1–M4) form the channel pore structure, with the five M2 domains directly lining the channel pore. The interface between the ECD and the TMD is termed the transition zone, which is formed by loop 2, the Cys-loop and the pre-M1 linker from the ECD side and the M2-M3 loop from the TMD side (5–10). Agonist-mediated channel activation involves a realignment of the transition zone, which in turn leads to a reconfiguration of the M2-M3 loop and the opening of the channel (11–15).

To ensure efficient channel activation, a precisely structured transition zone is required. A large body of studies has demonstrated that networks of energetic interactions between residues, especially between charged residues, exist throughout the transition zone (16, 17). These residue interactions have been shown to be essential for the transmission of agonist-induced conformational changes to the channel gate. However, to date,

* This study was supported by the Australian Research Council and the National Health and Medical Research Council of Australia.
[S] This article contains supplemental Figs. S1 and S2.
[1] To whom correspondence should be addressed: Brain and Mind Research Institute, University of Sydney, Sydney, NSW, 2050, Australia. Tel.: 61-2-9114-4032; Fax: 61-2-9114-4035; E-mail: qshan@yahoo.com.
[2] The abbreviations used are: GlyR, glycine receptor; nAChR, nicotinic acetylcholine receptor; $5HT_3R$, 5-hydroxytryptamine type 3 receptor; $GABA_AR$, type A γ-aminobutyric acid receptor; ECD, extracellular domain; TMD, transmembrane domain; ER, endoplasmic reticulum.

the mechanisms by which residue interactions affect surface expression have barely been investigated.

The GlyR is an integral protein, which is synthesized and assembled in the endoplasmic reticulum (ER), modified in the Golgi complex and eventually shipped into the cell membrane. Integral proteins are under stringent surveillance by the quality control machinery in the ER and, occasionally, in the Golgi complex, which ensures that only properly folded and assembled proteins are shipped to the cell membrane, whereas misfolded proteins are retained in the cytoplasm and eventually degraded (18–20).

Here we report that the incompatibility between a pair of residues, in close proximity to each other in the tertiary structure, but from the discrete pre-M1 and Cys-loop domains, prevents surface expression of the GlyR. We propose that this residue incompatibility (electrostatic repulsion) misfolds the GlyR protein, and in consequence, the protein is retained in the cytoplasm and prevented from further surface expression by the quality control machinery. This hypothesis suggests a novel mechanism for explaining mutation-induced reduction in channel surface expression, often present in the cases of hereditary hyperekplexia.

EXPERIMENTAL PROCEDURES

Mutagenesis and Chimera Construction of the GlyR cDNAs—The human GlyR α1 subunit cDNA was subcloned into the pcDNA3.1zeo+ plasmid vector (Invitrogen, Carlsbad, CA) for expression in HEK293 cells. Site-directed mutagenesis and chimera construction (including insertion of the DYKDDDDK FLAG tag between the Arg-2 and Ser-3 of the GlyR α1 sequence) were performed using the QuickChange (Stratagene, La Jolla, CA) mutagenesis and multiple-template-based sequential PCR protocols, respectively.

The multiple-template-based sequential PCR protocol for chimera construction was developed in our laboratory and has recently been described in detail elsewhere (21). This procedure does not require the existence of restriction sites, or the purification of intermediate PCR products, and needs only two or three simple PCRs followed by general subcloning steps. Most importantly, the chimera join sites are seamless, *i.e.* no linker sequence is required, and the success rate for construction is nearly 100%. The joining sites used in our experiment were chosen based on two criteria. First, the site, based on the crystal structure of the acetylcholine-binding protein (5), should be located near the boundary between the two flanking loops to minimize disturbance on the loop structures. Second, the pair of residues between which a joining site is formed should be conserved between the GlyR α and β subunits, if possible. The join sites used in our experiments were located between the following pairs of residues: α L134-T135 and β I157-T158 for the N terminus of the Cys-loop, α Q155-L156 and β Q178-L179 for the C terminus of the Cys-loop, α T208-C209 and β T232-C233 for the N terminus of the pre-M1 linker, and α G221-Y222 and β G245-F246 for the C terminus of the pre-M1 linker (supplemental Fig. S1).

HEK293 Cell Culture and Expression—Details of the HEK293 (ATCC, Manassas, VA) cell culture and GlyR expression are described elsewhere (22). Briefly, HEK293 cells were maintained in DMEM supplemented with 10% fetal bovine serum. Cells were transfected using a calcium phosphate precipitation protocol. In addition, the pEGFP-N1 plasmid vector (Clontech, Mountain View, CA) was co-transfected to facilitate identification of the transfected cells in electrophysiological recordings.

Electrophysiological Recording—An inverted fluorescence microscope was used to visualize cells for electrophysiological experiments. Cells expressing recombinant GlyRs were identified by their green fluorescence. Borosilicate glass capillary tubes (Vitrex, Modulohm, Denmark) and a horizontal pipette puller (P97, Sutter Instruments, Novato, CA) were used to pull patch clamp pipettes with tip resistances of 2–3 MΩ when filled with pipette solution containing (in mM): 145 CsCl, 2 $CaCl_2$, 2 $MgCl_2$, 10 HEPES, and 10 EGTA, adjusted to pH 7.4 with CsOH. Cells were perfused by an external solution containing (in mM): 140 NaCl, 5 KCl, 2 $CaCl_2$, 1 $MgCl_2$, 10 HEPES, and 10 D-glucose, adjusted to pH 7.4 with NaOH. Cells were voltage-clamped at −40 mV in the whole-cell recording configuration and membrane currents were recorded using an Axon Multiclamp 700B amplifier and pClamp 10 software (Molecular Devices, Sunnyvale, CA). Membrane currents were filtered at 500 Hz and digitized at 2 kHz. Stocks of glycine (1 M in the external solution) were maintained at −20 °C. Ivermectin (Sigma-Aldrich) was dissolved in dimethyl sulfoxide and stored as 10 mM stocks at −20 °C. Solutions were applied to cells via a gravity-induced perfusion systems fabricated from polyethylene tubing. All experiments were performed at room temperature (22–23 °C).

Immunofluorescence Imaging—HEK293 cells were grown on glass coverslips and transfected with FLAG-tagged constructs as described above. At 48 h after transfection, the cells were washed twice in ice-cold phosphate-buffered saline (PBS) solution. For surface staining, the cells were labeled with the mouse monoclonal anti-FLAG antibody (1 μg/ml, Cat No. F1804, Sigma-Aldrich) in ice-cold DMEM (with serum) on ice for 30 min and then washed three times in ice-cold PBS. The subsequent steps were performed at room temperature in the following order: cells were fixed using 4% paraformaldehyde in PBS for 20 min, permeabilized using 0.25% Triton 100 in PBS for 5 min, blocked using 10% BSA in PBS for 1 h, and labeled with the Alexa-Fluor-488-conjugated goat anti-mouse secondary antibody (2 μg/ml, Invitrogen) in 3% BSA/PBS in a dark place for 1 h. Cells were finally mounted in a mounting medium and imaged using a confocal microscope (LSM510 META, Zeiss). For total staining, the cells were treated at room temperature in an order slightly different from that used for surface staining: The cells were fixed, permeabilized, and blocked. The cells were subsequently labeled with anti-FLAG antibody in 3% BSA/PBS for 2 h, and with Alexa-Fluor-488-conjugated goat anti-mouse secondary antibody. Finally, the cells were mounted and imaged. All the manipulations and solution ingredients for total staining were the same as for surface staining unless specified above.

Data Analysis—Results are expressed as means ± S.E. of the mean of four or more independent experiments. The empirical Hill equation, fitted by a non-linear least squares algorithm

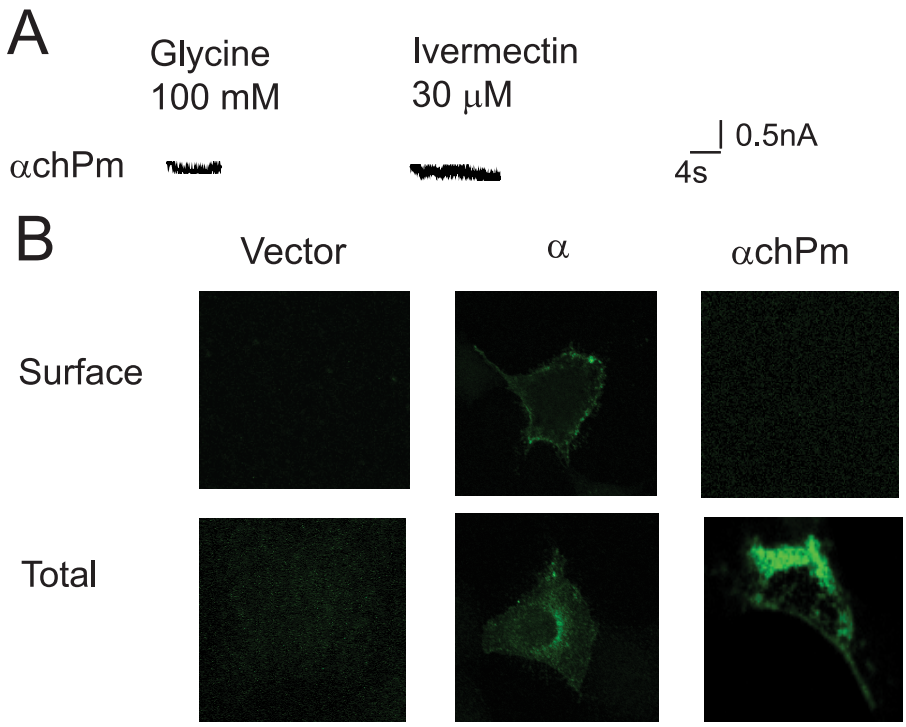

FIGURE 1. **Absence of surface expression in the αchPm GlyR.** *A*, sample traces of currents induced by glycine and ivermectin. *B*, surface and total staining of indicated constructs.

(SigmaPlot 9.0, Systat Software, Point Richmond, CA), was used to calculate the glycine EC_{50}.

RESULTS

Homologous Substitution of the Pre-M1 Linker from the β Subunit Blocks Surface Expression of the α1 GlyR—The GlyR exists in either homomeric α or heteromeric α β form. The β subunit alone cannot form homomeric channels. In an attempt to investigate the structural requirements for GlyR functional surface expression, we constructed several chimeras of α1 and β subunits. One of the chimeras, in which the pre-M1 linker in the α1 GlyR was replaced with the homologous domain from the β subunit (*αchPm*, Fig. 2*B* and supplemental Fig. S1) could not induce any current upon application of the agonist glycine at concentrations up to 100 mM (Fig. 1*A*). This could be due to compromised channel function or blocked surface expression.

To distinguish these two possibilities, we applied ivermectin to the αchPm GlyR. Ivermectin is a GlyR agonist, which binds to the receptor and gates the channel via a different mechanism from that of glycine (23, 24). It has been shown that ivermectin can induce currents in certain GlyRs with mutations that disrupt the glycine-activated channel gating pathway but leave surface expression intact (23). We wondered whether this was the case for the αchPm GlyR, as the pre-M1 linker is one of the essential components of the glycine-activated channel gating pathway (11–15). As shown in Fig. 1*A*, a saturating (30 μM) ivermectin concentration induced no current, implying that the αchPm GlyR might not be surface-expressed.

To verify this possibility, we directly examined the surface expression by immunofluorescence imaging. To achieve this, we inserted the FLAG tag into the N terminus of the αchPm subunit and labeled the receptor with the anti-FLAG antibody. As shown in Fig. 1*B*, the αchPm GlyR was detected in the cytoplasm but not on the cell surface. In contrast, the α1 GlyR tagged with the FLAG was detected not only in the cytoplasm but also on the cell surface. It is noteworthy that the FLAG tag insertion did not change the receptor and channel properties of the GlyR, as the glycine dose-current response curves of the α1 GlyRs with and without the FLAG tag overlapped (EC_{50}: 33 ± 2 μM, $n = 4$ without FLAG *versus* 34 ± 4 μM, $n = 4$ with FLAG, $p > 0.05$) (supplemental Fig. S2).

Homologous Substitution of the Cys-loop from the β Subunit Restores the Function of the αchPm GlyR—To investigate the structural basis on which α1 GlyR surface expression was blocked by the homologous substitution of the pre-M1 linker from the β subunit, we constructed two chimeras of the α1 and β subunits, which we termed αchEn and αchEc, respectively. They were constructed by replacing either the N terminus or the C terminus half, respectively, of the ECD in the α1 subunit, with the homologous sequence from the β subunit (Fig. 2*B* and supplemental Fig. S1). Because the N terminus of the β subunit contains motifs that block homomer formation (25, 26) (supplemental Fig. S1), we replaced these motifs with the homologous residues from the α subunit in the αchEn GlyR. This modified construct was able to form a functional homomeric channel (EC_{50} = 301 ± 26 μM, I_{max} = 9.6 ± 1.3 nA and $n = 4$, Fig. 2*C*), which is consistent with previous reports (25, 26). But surprisingly, the αchEc GlyR, which incorporated the pre-M1 linker, the Cys-loop, loops B, F, and C from the β subunit (supplemental Fig. S1), could also form a functional channel (EC_{50} = 46 ± 8 μM, I_{max} = 14.6 ± 1.7 nA and $n = 4$, Fig. 2*C*), with similar glycine sensitivity to the α1 GlyR (EC_{50} = 33 ± 2 μM, I_{max} = 6.6 ± 1.1 nA and $n = 4$, Fig. 2*C*). This was in sharp

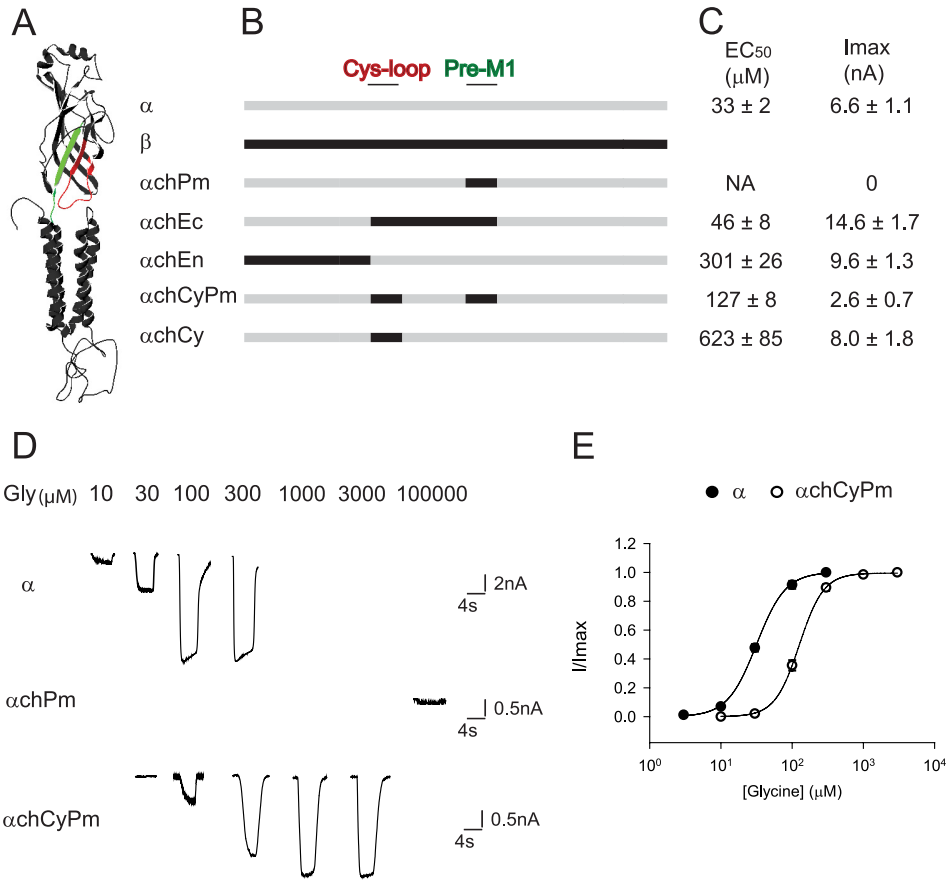

FIGURE 2. **Homologous substitution of the Cys-loop from the β subunit restores the function of the αchPm GlyR.** *A*, pre-M1 linker (*green*) and Cys-loop (*red*) are highlighted in a structural model of a single GlyR α1 subunit. Construction of chimeras is schematically illustrated in *B* and their glycine EC_{50} and I_{max} values are shown in *C* (NA, not applicable). Sample current traces and averaged normalized glycine dose-response curves of indicated constructs are shown in *D* and *E*, respectively.

contrast to the absence of surface expression in the αchPm GlyR, which incorporated only the pre-M1 linker from the β subunit. We thus concluded that the Cys-loop, loop B, F, or C of the β subunit restored the surface expression in the αchEc GlyR. We next investigated which of these domains was responsible for the restoration of surface expression in the αchEc GlyR.

Based on the primary sequence, loop C is linearly connected to the pre-M1 linker. However, based on the tertiary structures of various Cys-loop receptor superfamily members, the Cys-loop is located physically close to the pre-M1 linker (Fig. 2*A*) (5–10). Considering that functional studies have shown that residues in the pre-M1 linker and Cys-loop interact with each other and that these interactions are essential for channel gating (14, 27, 28), we hypothesized that the Cys-loop, but not loop C, might be the component that restored the surface expression in the αchEc GlyR. We tested this hypothesis by constructing the chimera αchCyPm GlyR, where the Cys-loop from the β subunit was introduced into the αchPm GlyR (Fig. 2*B*, supplemental Fig. S1). As hypothesized, glycine-induced currents were indeed detected in this construct (EC_{50} = 127 ± 8 μM, I_{max} = 2.6 ± 0.7 nA and n = 4), which indicated receptor and channel properties similar to those of the α1 GlyR (Fig. 2, *C*--*E*). We thus concluded that the Cys-loop from the β subunit, when introduced into the αchPm GlyR, restored surface expression. More interestingly, the chimera αchCy GlyR (Fig. 2*B*), where only the Cys-loop from the β subunit was introduced into the α1 GlyR, also induced currents upon glycine application (EC_{50} = 623 ± 85 μM, I_{max} = 8.0 ± 1.8 nA and n = 4) (Fig. 2*C*).

A Pair of Positively Charged Residues in the Pre-M1 Linker and Cys-loop Causes the Absence of Surface Expression—Based on the results of the αchPm and αchCyPm GlyRs, we concluded that an interaction between the pre-M1 linker and Cys-loop controls the surface expression of the GlyR. To identify the structural basis of this interaction at single-residue level, we mapped residues from both domains that are not conserved between the α1 and β subunits onto a structural model of the α1 subunit (Fig. 3, *A* and *B*) (29). By observing the physiochemical properties of residues and their proximity to each other in the tertiary structure, our attention was drawn to a pair of residues, residue 143 from the Cys-loop and residue 217 from the pre-M1 linker (Fig. 3, *A* and *C*). It was the positive-charged Lys-143 and Arg-217 (α1 subunit numbering) that were in the non-surface-expressed αchPm GlyR, while at least one positive-charged residue was missing in all other constructs with normal surface expression we had examined so far (Fig. 3*D*).

These two residues are physically close to each other in the tertiary structure (Fig. 3*C*), with their α-carbon atoms separated by 11.6 Å in our model structure. We thus hypothesized that the electrostatic repulsion between the two positive

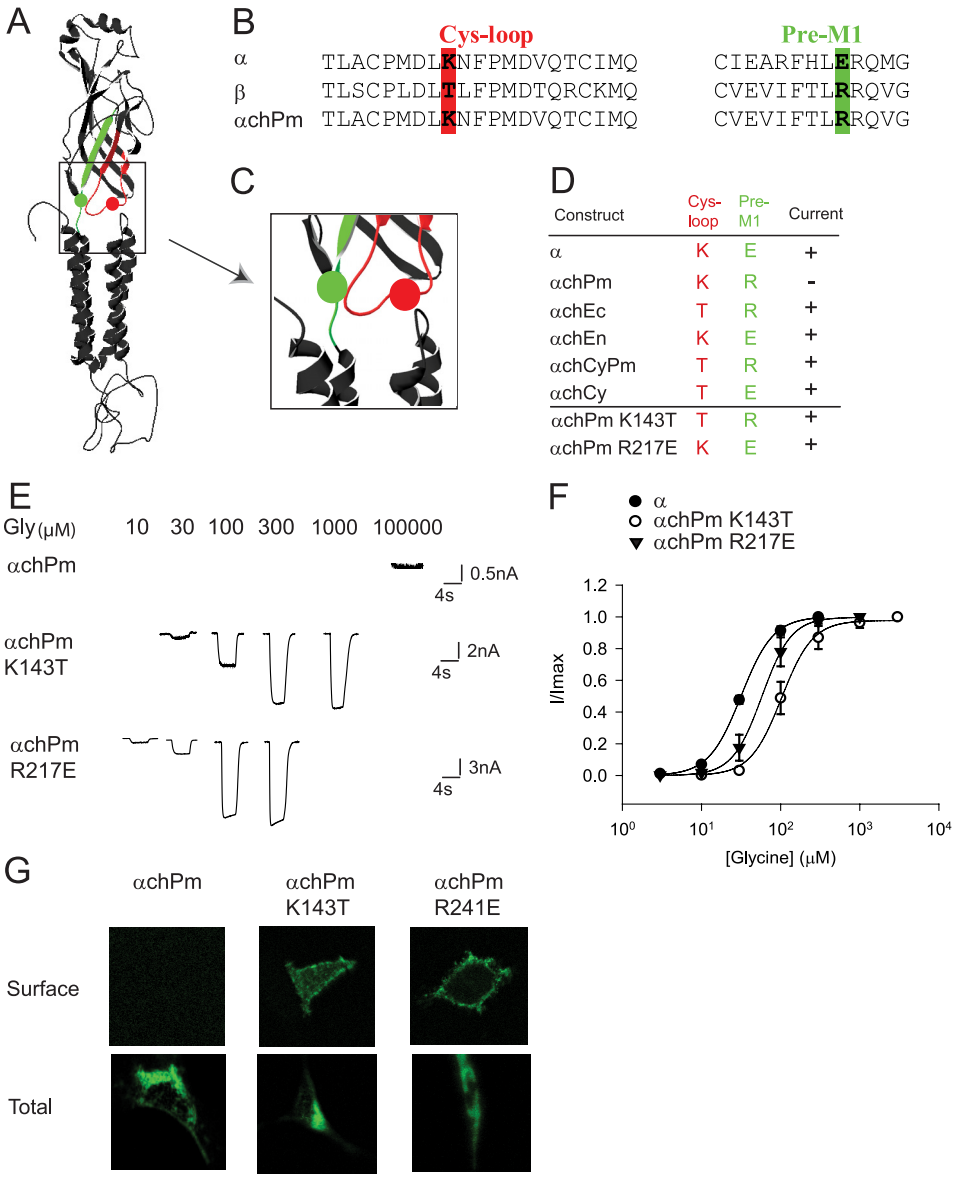

FIGURE 3. **Interaction of residues 143 and 217 affects surface expression of the GlyR.** *A*, pre-M1 linker (*green*) and Cys-loop (*red*) are highlighted in a structural model of the GlyR α1 subunit. *B*, sequences of the Cys-loop and pre-M1 linker of indicated constructs. Residues 143 and 217 are highlighted in *red* and *green*, respectively. *C*, local domain hosting residues 143 (*red ball*) and 217 (*green ball*) is shown in an enlarged section. *D*, amino acids at the 143 and 217 positions of indicated constructs and whether they induce current (+) or not (−) upon glycine application is shown. Sample current traces, averaged normalized glycine dose-response curves, and surface and total staining of indicated constructs are shown in *E*, *F*, and *G*, respectively.

charges was the cause for the absence of surface expression in the αchPm GlyR. If this were the case, substitution of K143T or R217E, either of which would eliminate any electrostatic repulsion, should restore surface expression of the αchPm GlyR, as in the αchCyPm and α1 GlyRs, respectively. As anticipated, both the αchPm K143T and αchPm R217E GlyRs induced current upon glycine application (EC_{50} = 117 ± 28 μM, Imax = 10.1 ± 4.1 nA, n = 4 and EC_{50} = 62 ± 13 μM, Imax = 9.9 ± 3.7 nA, n = 4, respectively, Fig. 3, *D--F*). Moreover, surface expression of both constructs was also confirmed by immunofluorescence imaging (Fig. 3*G*). We therefore concluded that an electrostatic interaction (electrostatic repulsion) between the Lys-143 residue from the Cys-loop and the Arg-217 residue from the pre-M1 linker blocks surface expression of the αchPm GlyR. In other words, compatibility between this pair of residues from the pre-M1 linker and Cys-loop is essential for surface expression of the GlyR.

DISCUSSION

Mutations of Charged Residues in the Transition Zone Block Surface Expression—Here we demonstrate that interaction between a pair of positively charged residues from the Cys-loop and pre-M1 linker blocks surface expression of the GlyR. Because these two residues are in close proximity to each other in the tertiary structure, we propose that electrostatic repulsion between them is responsible for lack of surface expression. It should be noted that, although this seems a likely mechanism, we could not eliminate the possibility that the co-existence of Lys-243 and Arg-217 could cause conformational changes other than electrostatic repulsion, which lead to failure of surface expression.

It should be noted that the repulsion we propose here could exist between Lys-143 and Arg-217 within one subunit or between Lys-143 in one subunit and Arg-217 in an adjacent subunit. However, we think the latter case is less likely because in the heteromeric $\alpha\beta$ GlyR, the α and β subunits are supposed to be adjacent to each other but the α subunit carries a Lys-143 while the β subunit carries an Arg-217 (α numbering) (Fig. 3*B*). Yet the $\alpha\beta$ GlyR is still surface-expressed properly, based on multiple previous reports (22, 30–32).

The GlyR is an allosteric protein, which requires a precisely organized transition zone to build a signaling pathway for transmitting the ligand-binding information to the channel gate. Previous studies have demonstrated that several interactions between pairs of oppositely charged residues exist throughout this signaling pathway and that these interactions mediate the channel gating information flow (16, 17). However, the results presented here imply that proper residue interaction also affects surface expression. It has previously been reported that mutations of single charged residues in the transition zone block surface expression in Cys-loop receptor superfamily members (33–36). For example, the hyperekplexia-causing R218Q mutation, located at the pre-M1 linker in the α1 GlyR, caused a marked decrease in surface receptor expression (35). In addition, mutations of positively charged residues homologous to the Arg-218 of the GlyR α1 subunit also reduced surface expression of receptors incorporating $GABA_AR$ α1 (36), $GABA_AR$ ρ1 (33, 34) and $5HT_3R$ A (33) subunits. This implies that proper interaction between charged residues and other residues, at least at the pre-M1 linker, might be an essential factor determining surface expression of the Cys-loop receptors.

As noted above, Cys-loop receptor superfamily members share common structural and functional characteristics. If compatibility between the 143 and 217 residues is essential for surface expression of the GlyR, we wondered whether this rule applies more widely in the Cys-loop receptor superfamily. By comparing the homologous residues in other Cys-loop receptor subunits, we noticed that most of them, with few exceptions, are compatible with each other due to the non-existence of a pair of positively charged residues at the two positions (Fig. 4). The exceptions to this are the nAChR α7, β2, β4, and the $GABA_AR$ β1–3 subunits, where positively charged residues do exist at the two positions (Fig. 4). We suggest that this may be explained by structural variations among Cys-loop receptor superfamily members. Indeed, this has been suggested by previous studies seeking to explain how channel gating is affected by charged residues in the transition zone (37, 38). For example, in the $GABA_AR$ β2 subunit, the positively charged Lys, which is equivalent to the 217 residue in the GlyR α1 subunit, has been shown to interact with three negatively charged residues in the vicinity of the positively charged Arg, equivalent to the 143 residue in GlyR α1 subunit (27). These three negatively charged residues might shield the two positively charged residues from direct interaction and ensure proper folding and subsequent surface expression of the protein.

Possible Mechanism Underlying Incompatibility between Residues Blocking Surface Expression—Absence of protein surface expression is often attributed to ER retention. Conversion

nAChR α1	CEIIV**T**HFPFDEQNC	**Q**RLPL
nAChR α2	CSIDV**T**FFPFDQQNC	**R**RLPL
nAChR α3	CKIDV**T**YFPFDYQNC	**R**RLPL
nAChR α4	CSIDV**T**FFPFDQQNC	**R**RLPL
nAChR α5	CTIDV**T**FFPFDLQNC	**K**RLPL
nACHR α6	CPMDI**T**FFPFDHQNC	**R**RLPM
nACHR α7	CYIDV**R**WFPFDVQHC	**R**RRTL
nAChR α9	CVVDV**T**YFPFDNQQC	**K**RRSS
nAChR α10	CRVDV**A**AFPFDAQHC	**R**RRAA
nAChR β1	CSIQV**T**YFPFDWQNC	**R**RKPL
nAChR β2	CKIEV**K**HFPFDQQNC	**R**RKPL
nAChR β3	CTMDV**T**FFPFDRQNC	**R**RLPL
nAChR β4	CKIEV**K**YFPFDQQNC	**K**RKPL
nAChR δ	CPISV**T**YFPFDWQNC	**R**RKPL
nAChR ε	CAVEV**T**YFPFDWQNC	**R**RKPL
nAChR γ	CSISV**T**YFPFDWQNC	**Q**RKPL
5HT3R A	CSLDI**Y**NFPFDVQNC	**R**RRPL
5HT3R B	CSLET**Y**AFPFDVQNC	**R**RHPL
5HT3R C	CNLDI**F**YFPFDQQNC	**R**RRPS
5HT3R E	CNLDI**F**YFPFDQQNC	**R**RRPS
GABAaR α1 *	CPMHL**E**DFPMDAHAC	**K**RKIG
GABAaR α2 *	CPMHL**E**DFPMDAHSC	**K**RKIG
GABAaR α3 *	CPMHL**E**DFPMDVHAC	**K**RKIG
GABAaR α4	CPMRL**V**DFPMDGHAC	**R**RKMG
GABAaR α5 *	CPMQL**E**DFPMDAHAC	**K**RKIG
GABAaR α6	CPMRL**V**NFPMDGHAC	**Q**RKMG
GABAaR β1	CMMDL**R**RYPLDEQNC	**K**RNIG
GABAaR β2	CMMDL**R**RYPLDEQNC	**K**RNIG
GABAaR β3	CMMDL**R**RYPLDEQNC	**K**RNIG
GABAaR γ1	CYLQL**H**NFPMDEHSC	**S**RRMG
GABAaR γ2	CQLQL**H**NFPMDEHSC	**S**RRMG
GABAaR γ3	CQLQL**H**NFPMDEHSC	**S**RRMG
GABAaR γ4	CSLHM**L**RFPMDSHSC	**S**RRFG
GABAaR τ	CSLDL**H**KFPMDKQAC	**Q**REVN
GABAaR δ	CDMDL**A**KYPMDEQEC	**R**RNRG
GABAaR π	CNMDL**S**KYPMDTQTC	**R**RNVL
GABAaR ε	CSLHM**L**RFPMDSHSC	**S**RRFG
GABAaR ρ1	CNMDF**S**RFPLDTQTC	**R**RHIF
GABAaR ρ2	CNMDF**S**HFPLDSQTC	**R**RHIF
GABAaR ρ3	CFMDF**S**RFPLDTQNC	**R**RHVF
GlyR α1 *	CPMDL**K**NFPMDVQTC	**E**RQMG
GlyR α2 *	CPMDL**K**NFPMDVQTC	**E**RQMG
GlyR α3 *	CPMDL**K**NFPMDVQTC	**E**RQMG
GlyR α4 *	CLMDL**K**NFPMDIQTC	**E**RQMG
GlyR β	CPLDL**T**LFPMDTQRC	**R**RQVG

FIGURE 4. **Amino acid sequence alignment of the Cys-loops and pre-M1 linkers among members of the Cys-loop receptor superfamily.** Residues equivalent to the 143 and 217 residues in the GlyR α1 subunit are highlighted in *bold*. Cys-loop receptor superfamily members with a pair of positively charged or oppositely charged residues, at positions equivalent to the 143 and 217 residues in the GlyR α1 subunit, are *underlined* or marked with *asterisks*, respectively.

to ER retention from surface expression is usually caused by introduction of new, or exposure of originally hidden, ER retention signals (18–20, 39). The non-surface-expressed αchPm GlyR, compared with the surface-expressed α GlyR, incorporated an Arg residue at the 217 position, thus forming an RR sequence together with the Arg-218. The RR sequence serves as an ER retention signal in some proteins, such as 3-hydroxy-3-methylglutaryl-coezyme A reductase and GPI-anchor biosynthesis protein, but only when the signal exists in the very N terminus of proteins (39). Therefore, it is unlikely that a new ER retention signal was introduced in the αchPm GlyR.

Instead, we propose that incompatibility between the pair of positively charged residues from the Cys-loop and pre-M1 linker distorts the global structure of the αchPm GlyR. As a result, this distorted (or misfolded) protein is prevented from surface expression by quality control machinery within the cell.

As noted above, the transition zone is formed by loop 2, the Cys-loop, pre-M1 linker, and M2-M3 loop, none of which are covalently connected with each other. These four components must be precisely organized with each other to faithfully transmit the channel activation information from the agonist binding site to the channel gate (6–10). Incompatibility between residues within a precisely organized region likely causes a large pressure on the global structure of a protein. In the case of the achPm GlyR, the positively charged 217 residue is buried in the precisely organized transition zone. When a residue with the same charge is introduced in close proximity, electrostatic repulsion might occur between the pair of residues, which in consequence might distort the local and even global structure of the GlyR protein.

Proper protein folding is essential for subsequent binding of trafficking chaperon proteins and interacting with other subunits on the way to the cell membrane, whereas misfolded proteins would likely be retained in the ER or Golgi complex through its quality control machinery and eventually degraded (19, 20). For example, the N470D mutation in the ERG potassium channel blocks surface expression by ER retention (40). The underlying mechanism is that this mutation misfolds the protein, thus prolongs association with chaperon proteins and in consequence restrains surface expression (41). Moreover, the ER quality control machinery coupled with the ubiquitin-proteasome system has been shown to regulate surface expression of the GlyR and nAChR (42–44).

Contribution to Channel Gating—Like several other pairs of residues with opposite charges in the transition zone, Lys-143 and Glu-217 in the GlyR might also directly couple with each other and contribute to the channel gating pathway. However, we were unable to determine whether this was the case because the lack of surface expression of the αchPm GlyR prevented us from measuring its glycine EC_{50} and, as a result, we could not employ mutant cycle analysis to infer whether an energetic coupling exists between these two residues. Direct coupling between these respective homologous residues has not yet been reported in any other Cys-loop receptor member. It should be noted that the homologous pairs of residues are oppositely charged in only a few of the Cys-loop receptor superfamily members, *i.e.* the $GABA_AR$ α1, α2, α3, and α5, and GlyR α1, α2, α3, and α4 subunits (Fig. 4). Interestingly, the residues homologous to the GlyR α1 143 and 217 are negatively and positively charged, respectively, in these $GABA_AR$ α subunits, which is the reverse of that in GlyR α subunits (Fig. 4). This implies that these oppositely charged residues can be swapped with each other while maintaining receptor-gated channel function. This phenomenon is typical of other pairs of oppositely charged residues that couple with each other and form the channel gating pathway in the transition zone.

CONCLUSION

In this article, we demonstrate that homologous substitution of the pre-M1 linker from the β subunit blocks surface expression of the α1 GlyR. This effect is due to interaction of a pair of positively charged residues, in close proximity to each other in the tertiary structure, from the pre-M1 linker and Cys-loop. Abolishing either positive charge restores surface expression. We propose that an electrostatic repulsion between this pair of residues is responsible for the failure of surface expression. This hypothesis suggests a novel mechanism, *i.e.* residue incompatibility, for explaining mutation-induced reduction in channel surface expression, often present in the cases of hereditary hyperekplexia.

Acknowledgment—We thank J. Mullins (Swansea University, UK) for kindly sharing with us the structural model of the GlyR α1 subunit.

REFERENCES

1. Harvey, R. J., Topf, M., Harvey, K., and Rees, M. I. (2008) The genetics of hyperekplexia: more than startle! *Trends Genet.* **24,** 439–447
2. Lynch, J. W. (2004) Molecular structure and function of the glycine receptor chloride channel. *Physiol. Rev.* **84,** 1051–1095
3. Miller, P. S., and Smart, T. G. (2010) Binding, activation and modulation of Cys-loop receptors. *Trends Pharmacol. Sci.* **31,** 161–174
4. Thompson, A. J., Lester, H. A., and Lummis, S. C. (2010) The structural basis of function in Cys-loop receptors. *Q. Rev. Biophys.* **43,** 449–499
5. Brejc, K., van Dijk, W. J., Klaassen, R. V., Schuurmans, M., van Der Oost, J., Smit, A. B., and Sixma, T. K. (2001) Crystal structure of an ACh-binding protein reveals the ligand-binding domain of nicotinic receptors. *Nature* **411,** 269–276
6. Bocquet, N., Nury, H., Baaden, M., Le Poupon, C., Changeux, J. P., Delarue, M., and Corringer, P. J. (2009) X-ray structure of a pentameric ligand-gated ion channel in an apparently open conformation. *Nature* **457,** 111–114
7. Hilf, R. J., and Dutzler, R. (2009) Structure of a potentially open state of a proton-activated pentameric ligand-gated ion channel. *Nature* **457,** 115–118
8. Hilf, R. J., and Dutzler, R. (2008) X-ray structure of a prokaryotic pentameric ligand-gated ion channel. *Nature* **452,** 375–379
9. Unwin, N. (2005) Refined structure of the nicotinic acetylcholine receptor at 4A resolution. *J. Mol. Biol.* **346,** 967–989
10. Hibbs, R. E., and Gouaux, E. (2011) Principles of activation and permeation in an anion-selective Cys-loop receptor. *Nature* **474,** 54–60
11. Purohit, P., Mitra, A., and Auerbach, A. (2007) A stepwise mechanism for acetylcholine receptor channel gating. *Nature* **446,** 930–933
12. Grosman, C., Zhou, M., and Auerbach, A. (2000) Mapping the conformational wave of acetylcholine receptor channel gating. *Nature* **403,** 773–776
13. Bouzat, C., Gumilar, F., Spitzmaul, G., Wang, H. L., Rayes, D., Hansen, S. B., Taylor, P., and Sine, S. M. (2004) Coupling of agonist binding to channel gating in an ACh-binding protein linked to an ion channel. *Nature* **430,** 896–900
14. Lee, W. Y., Free, C. R., and Sine, S. M. (2009) Binding to gating transduc-

tion in nicotinic receptors: Cys-loop energetically couples to pre-M1 and M2-M3 regions. *J. Neurosci.* **29,** 3189–3199
15. Lummis, S. C., Beene, D. L., Lee, L. W., Lester, H. A., Broadhurst, R. W., and Dougherty, D. A. (2005) Cis-trans isomerization at a proline opens the pore of a neurotransmitter-gated ion channel. *Nature* **438,** 248–252
16. Cederholm, J. M., Schofield, P. R., and Lewis, T. M. (2009) Gating mechanisms in Cys-loop receptors. *Eur. Biophys. J.* **39,** 37–49
17. Chang, Y. C., Wu, W., Zhang, J. L., and Huang, Y. (2009) Allosteric activation mechanism of the Cys-loop receptors. *Acta Pharmacol. Sin.* **30,** 663–672
18. Ellgaard, L., and Helenius, A. (2003) Quality control in the endoplasmic reticulum. *Nat. Rev. Mol. Cell Biol.* **4,** 181–191
19. Ellgaard, L., Molinari, M., and Helenius, A. (1999) Setting the standards: quality control in the secretory pathway. *Science* **286,** 1882–1888
20. Ma, D., Taneja, T. K., Hagen, B. M., Kim, B. Y., Ortega, B., Lederer, W. J., and Welling, P. A. (2011) Golgi export of the Kir2.1 channel is driven by a trafficking signal located within its tertiary structure. *Cell* **145,** 1102–1115
21. Shan, Q., and Lynch, J. W. (2010) Chimera construction using multiple-template-based sequential PCRs. *J. Neurosci. Methods* **193,** 86–89
22. Shan, Q., Haddrill, J. L., and Lynch, J. W. (2001) A single β-subunit M2 domain residue controls the picrotoxin sensitivity of αβ heteromeric glycine receptor chloride channels. *J. Neurochem.* **76,** 1109–1120
23. Shan, Q., Haddrill, J. L., and Lynch, J. W. (2001) Ivermectin, an unconventional agonist of the glycine receptor chloride channel. *J. Biol. Chem.* **276,** 12556–12564
24. Pless, S. A., Dibas, M. I., Lester, H. A., and Lynch, J. W. (2007) Conformational variability of the glycine receptor M2 domain in response to activation by different agonists. *J. Biol. Chem.* **282,** 36057–36067
25. Griffon, N., Büttner, C., Nicke, A., Kuhse, J., Schmalzing, G., and Betz, H. (1999) Molecular determinants of glycine receptor subunit assembly. *EMBO J.* **18,** 4711–4721
26. Kuhse, J., Laube, B., Magalei, D., and Betz, H. (1993) Assembly of the inhibitory glycine receptor: identification of amino acid sequence motifs governing subunit stoichiometry. *Neuron* **11,** 1049–1056
27. Kash, T. L., Dizon, M. J., Trudell, J. R., and Harrison, N. L. (2004) Charged residues in the β2 subunit involved in GABAA receptor activation. *J. Biol. Chem.* **279,** 4887–4893
28. Lee, W. Y., and Sine, S. M. (2005) Principal pathway coupling agonist binding to channel gating in nicotinic receptors. *Nature* **438,** 243–247
29. Chung, S. K., Vanbellinghen, J. F., Mullins, J. G., Robinson, A., Hantke, J., Hammond, C. L., Gilbert, D. F., Freilinger, M., Ryan, M., Kruer, M. C., Masri, A., Gurses, C., Ferrie, C., Harvey, K., Shiang, R., Christodoulou, J., Andermann, F., Andermann, E., Thomas, R. H., Harvey, R. J., Lynch, J. W., and Rees, M. I. (2010) Pathophysiological mechanisms of dominant and recessive GLRA1 mutations in hyperekplexia. *J. Neurosci.* **30,** 9612–9620
30. Grudzinska, J., Schemm, R., Haeger, S., Nicke, A., Schmalzing, G., Betz, H., and Laube, B. (2005) The β-subunit determines the ligand binding properties of synaptic glycine receptors. *Neuron* **45,** 727–739
31. Shan, Q., Han, L., and Lynch, J. W. (2011) β Subunit M2-M3 loop conformational changes are uncoupled from α1β glycine receptor channel gating: implications for human hereditary hyperekplexia. *PLoS ONE* **6,** e28105
32. Shan, Q., Nevin, S. T., Haddrill, J. L., and Lynch, J. W. (2003) Asymmetric contribution of α and β subunits to the activation of alphabeta heteromeric glycine receptors. *J. Neurochem.* **86,** 498–507
33. Price, K. L., Millen, K. S., and Lummis, S. C. (2007) Transducing agonist binding to channel gating involves different interactions in 5-HT3 and GABAC receptors. *J. Biol. Chem.* **282,** 25623–25630
34. Wang, J., Lester, H. A., and Dougherty, D. A. (2007) Establishing an ion pair interaction in the homomeric rho1 γ-aminobutyric acid type A receptor that contributes to the gating pathway. *J. Biol. Chem.* **282,** 26210–26216
35. Castaldo, P., Stefanoni, P., Miceli, F., Coppola, G., Del Giudice, E. M., Bellini, G., Pascotto, A., Trudell, J. R., Harrison, N. L., Annunziato, L., and Taglialatela, M. (2004) A novel hyperekplexia-causing mutation in the pre-transmembrane segment 1 of the human glycine receptor α1 subunit reduces membrane expression and impairs gating by agonists. *J. Biol. Chem.* **279,** 25598–25604
36. Mercado, J., and Czajkowski, C. (2006) Charged residues in the α1 and β2 pre-M1 regions involved in GABAA receptor activation. *J. Neurosci.* **26,** 2031–2040
37. Sala, F., Mulet, J., Sala, S., Gerber, S., and Criado, M. (2005) Charged amino acids of the N-terminal domain are involved in coupling binding and gating in α7 nicotinic receptors. *J. Biol. Chem.* **280,** 6642–6647
38. Xiu, X., Hanek, A. P., Wang, J., Lester, H. A., and Dougherty, D. A. (2005) A unified view of the role of electrostatic interactions in modulating the gating of Cys-loop receptors. *J. Biol. Chem.* **280,** 41655–41666
39. Teasdale, R. D., and Jackson, M. R. (1996) Signal-mediated sorting of membrane proteins between the endoplasmic reticulum and the Golgi apparatus. *Annu. Rev. Cell Dev. Biol.* **12,** 27–54
40. Zhou, Z., Gong, Q., and January, C. T. (1999) Correction of defective protein trafficking of a mutant HERG potassium channel in human long QT syndrome. Pharmacological and temperature effects. *J. Biol. Chem.* **274,** 31123–31126
41. Gong, Q., Jones, M. A., and Zhou, Z. (2006) Mechanisms of pharmacological rescue of trafficking-defective hERG mutant channels in human long QT syndrome. *J. Biol. Chem.* **281,** 4069–4074
42. Büttner, C., Sadtler, S., Leyendecker, A., Laube, B., Griffon, N., Betz, H., and Schmalzing, G. (2001) Ubiquitination precedes internalization and proteolytic cleavage of plasma membrane-bound glycine receptors. *J. Biol. Chem.* **276,** 42978–42985
43. Christianson, J. C., and Green, W. N. (2004) Regulation of nicotinic receptor expression by the ubiquitin-proteasome system. *EMBO J.* **23,** 4156–4165
44. Villmann, C., Oertel, J., Melzer, N., and Becker, C. M. (2009) Recessive hyperekplexia mutations of the glycine receptor α1 subunit affect cell surface integration and stability. *J. Neurochem.* **111,** 837–847

Incompatibility between a Pair of Residues from the Pre-M1 Linker and Cys-loop Blocks Surface Expression of the Glycine Receptor

Qiang Shan and Joseph W. Lynch

J. Biol. Chem. 2012, 287:7535-7542.
doi: 10.1074/jbc.M111.325126 originally published online January 20, 2012
